Advances in Geo-Energy Research

Vol. 22, No. 3, p. 201-214, 2026

Invited review

Multiscale heterogeneity in low permeability reservoirs: An integrated framework for characterization, quantification, and scale transfer

Ye Li[1,2], Gang Hui[1]*, Zhiyang Pi[2], Zhangxin Chen[3], Jing Li[1,2], Jianchao Cai[1]

[1]*State Key Laboratory of Petroleum Resources and Engineering, China University of Petroleum, Beijing 102249, P. R. China*

[2]*College of Petroleum Engineering, China University of Petroleum, Beijing 102249, P. R. China*

[3]*Ningbo Key Laboratory of Low Carbon Hydrogen Energy, Eastern Institute of Technology, Ningbo 315200, P. R. China*

Keywords:
Low permeability reservoir
multiscale heterogeneity
pore structure
upscaling
nonlinear flow
integrated framework

Cited as:
Li, Y., Hui, G., Pi, Z., Chen, Z., Li, J., Cai, J. Multiscale heterogeneity in low permeability reservoirs: An integrated framework for characterization, quantification, and scale transfer. Advances in Geo-Energy Research, 2026, 22(3): 201-214.
https://doi.org/10.46690/ager.2026.12.01

Abstract:
Low permeability reservoirs contain pore-throat systems spanning nanometers to kilometers. Their storage capacity, flow behavior, and development response therefore depend on scale. Homogeneous medium models cannot adequately represent this heterogeneity or transfer pore scale mechanisms to reservoir scale predictions. This study synthesizes methods for characterizing and quantifying heterogeneity and transferring information across scales. It distinguishes three genetic controls: Sedimentation, diagenesis, and tectonic deformation. Characterization methods are compared by measurement principle, resolution, and sampling volume. Fractal analysis, geostatistics, and digital core modeling are assessed as sources of quantitative descriptors. A published tight sandstone example illustrates data selection, cross calibration, pore scale indicators, and the transfer of core measurements to dynamic model inputs. Transferable mechanisms are distinguished from reservoir specific parameters because pore geometry and dominant flow processes vary among sandstone, shale, carbonate, and fractured systems. This study identifies four key research bottlenecks: Cross method calibration, physically consistent nonlinear upscaling, dynamic heterogeneity, and limited experimental and computational coverage. Priorities are uncertainty aware data integration, flow linked indicators, coupled dynamic validation, and efficient multiscale modeling. A unified research framework integrating characterization, quantification, and cross scale transfer is established. The findings provide a theoretical reference for microscopic pore-throat flow analysis and macroscopic dynamic prediction, as well as guidance for the efficient development of low permeability reservoirs.

1. Introduction

As conventional oil and gas resources decline, low permeability, ultra low permeability, and tight reservoirs have become important targets for reserve replacement and production growth. Unconventional oil and gas accounted for 23% of total hydrocarbon production in 2019 (Li et al., 2022a). The principal constraint on the efficient development of these reservoirs is severe multiscale heterogeneity, which controls pore connectivity, fluid mobility, and the reliability of reservoir scale prediction (Jia et al., 2012; Wang et al., 2016; Jia, 2017). Multiscale heterogeneity increases uncertainty in reservoir evaluation and development design. In tight sandstone gas reservoirs, matrix and fracture heterogeneity can make horizontal well parameter inversion nonunique (Kulga et al., 2018). History matching may be inefficient, while neural network estimates remain sensitive to nonuniqueness and data coverage

Yandy Scientific Press

*Corresponding author.
E-mail address: lypxszd@163.com (Y. Li); hui.gang@cup.edu.cn (G. Hui); pizhiyang1672@163.com (Z. Pi); zxchen@eitech.edu.cn (Z. Chen); lijingsuc@cup.edu.cn (J. Li); caijc@cup.edu.cn (J. Cai).
2207-9963 © The Author(s) 2026.
Received September 2, 2026; revised September 29, 2026; accepted October 16, 2026; available online October 20, 2026.

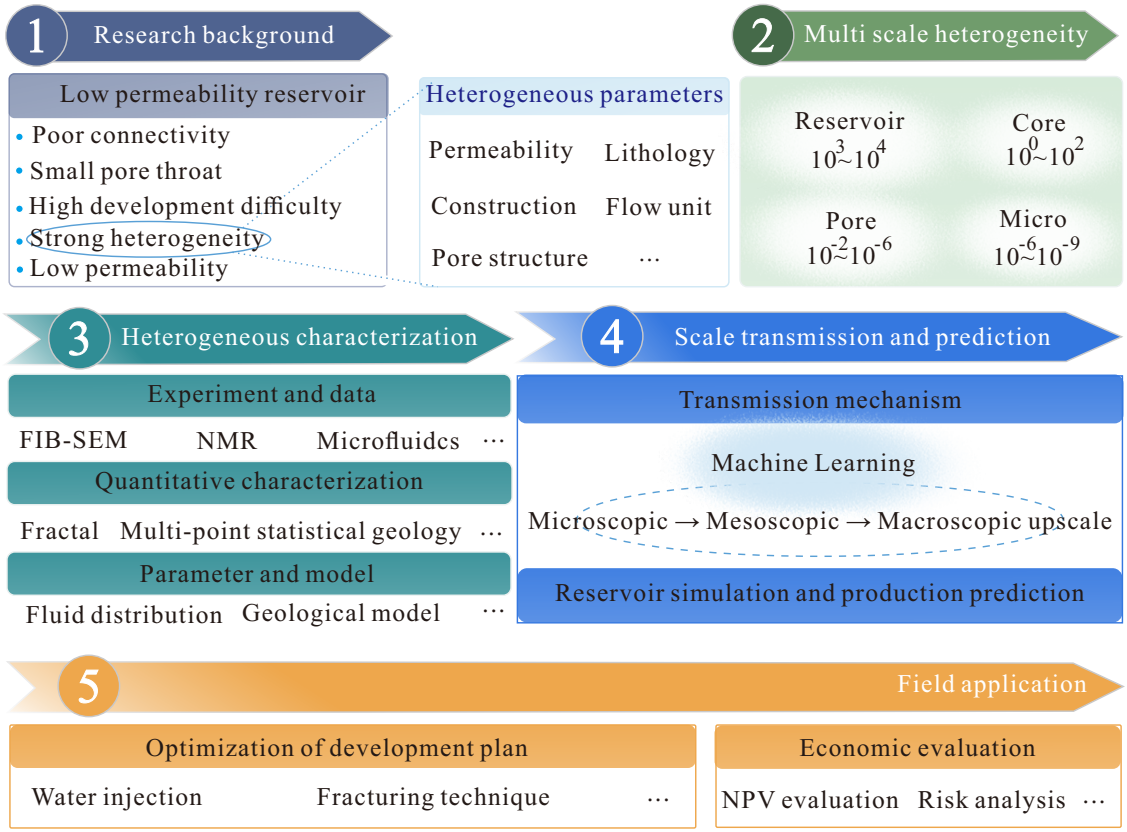


Fig. 1. Overall framework of multiscale heterogeneity research in low permeability reservoirs.

(Farhoodi et al., 2019; Hui et al., 2021; Li et al., 2025b). These issues also affect fractured vuggy carbonate development, CO_2 and hydrogen storage, and geothermal operations, where heterogeneity complicates monitoring and injection/production planning (Ren and Trevisan, 2020; Xu et al., 2022).

At pore scale, surface and boundary effects influence flow. At core scale, pore topology controls mobility, while at reservoir scale, sedimentary architecture and fractures shape flow pathways (Qiao et al., 2022). These scale dependent effects challenge continuum and Darcy flow assumptions. Multiscale modeling links pore scale imaging and flow simulation with reservoir scale upscaling (Durlofsky, 1998; Gerritsen and Durlofsky, 2005; Bultreys et al., 2016). Recent studies have further examined digital rock modeling, deep learning assisted pore imaging, and the effects of unresolved porosity on multiphase flow (Sadeghnejad et al., 2021; Wang et al., 2021). This study revolves around two main topics: The characterization and quantification of multiscale heterogeneity, and the transfer of pore scale information to engineering models while preserving the dominant flow mechanisms.

This study links reservoir geology, petrophysics, and engineering. It focuses on pore structure characterization, heterogeneity quantification, representative elementary volume (REV) analysis, upscaling, and nonlinear flow transfer. The workflow in Fig. 1 links the research background and the adverse effects on development, genetic origins of multiscale heterogeneity, experimental and quantitative characterization, and scale transfer mechanisms, and finally extends to reservoir simulation, production prediction, and field application. Studies were screened for (i) characterization methods and quantitative heterogeneity descriptors in low permeability, tight, shale, carbonate, or fractured reservoirs; (ii) REV, homogenization, or pore/core to reservoir transfer; and (iii) implications for production, carbon capture, utilization, and storage, underground gas storage, geothermal energy, or artificial intelligence assisted modeling (Hui et al., 2025). Table 1 summarizes the framework. The workflow may transfer across formations, but pore size distributions, wettability, fracture connectivity, and flow regimes require lithology and site specific calibration.

2. Multiscale heterogeneity in reservoirs

2.1 Genetic controls on heterogeneity

Sedimentation, diagenesis, and tectonic deformation generate heterogeneity across nested spatial scales, from pore systems to reservoir architecture. Sedimentation is a primary control on reservoir heterogeneity. Fluctuations in flow energy and provenance produced alternating delta front channels, mouth bars, and sheet sands. Sand body thickness, median grain size, and sorting coefficients vary by 40%-80%. These observations indicate that depositional energy and provenance create spatially variable textures; the petrophysical consequence is that coarser, better sorted channel sands tend to preserve more primary intergranular pores than clay rich deposits (Veloso et al., 2016). This inherited pore contrast is

Table 1. Integrated framework linking characterization, quantification, and scale transfer across scales.

Scale transition	Data	Descriptor	Transfer / uncertainty
Pore to core	SEM, FIB-SEM, microfluidics	Pore size; surface area; fractal dimension	Pore-throat flow; connectivity limits
Core to REV	CT, NMR, HPMI, core tests	Connectivity; tortuosity; movable fluid; REV	Effective flow; REV and stress uncertainty
Well to interwell	Logs; tests; tracers; seismic	Porosity; flow units; connectivity	Reservoir model; resolution mismatch
Reservoir to decision	Models; simulation; production data	Permeability; pressure/stress response	Production; CCUS/UGS; upscaling uncertainty

Notes: Carbon capture, utilization, and storage (CCUS); underground gas storage (UGS).

Table 2. Six level spatial scale hierarchy of heterogeneity in low permeability reservoirs.

Scale	Range	Heterogeneity type	Controlling factor
Nanopore	< 1 μm	Diagenetic	Clay minerals, organic matter
Micropore	μm-mm	Diagenetic/ Sedimentation	Grain arrangement, cementation
Core	cm	Diagenetic/ Microfractures	Differential cementation, microfractures
REV	dm-m	Sedimentation/ Fractures	Sedimentary microfacies, fracture
Interwell	10-100 m	Sedimentation	Sandbody distribution, facies transition
Reservoir	> 100 m	Sedimentation/ Tectonics	Basin evolution, faults

subsequently modified by compaction, cementation, and dissolution (Xi et al., 2019; Malki et al., 2023; Alkareemawi et al., 2025), whose effects vary with mineral composition, pore fluid chemistry, and burial conditions.

Tectonic deformation and diagenesis also generate fractures from microscopic cracks to field scale zones; together with matrix pores, these may form dual porosity flow networks (Correia et al., 2017; Li et al., 2025a, 2026b). Fracture density, orientation, aperture, and connectivity are lithology and structure dependent, so their effects on permeability and matrix fracture exchange require local characterization (Kim and Schechter, 2009; Li et al., 2021; Su et al., 2022). The three genetic controls interact across scales and should not be assigned individually to a single scale.

2.2 Hierarchical structure of multiscale heterogeneity

Scale transfer links measurements and models across these levels. Table 2 gives operational definitions. The three genetic controls are observed across six nested spatial levels: Nanopore, micropore and pore-throat, core, REV, interwell, and reservoir. These levels provide an organizing scheme rather than universal physical boundaries. The relevant scale depends on lithology, connectivity, fracture extent, and the measurement or modeling objective (Lu et al., 2024). Fig. 2 shows the spatial hierarchy of heterogeneity from pore to reservoir scales, illustrated by representative observations including focused ion beam-scanning electron microscopy (FIB-SEM), digital cores, well logs, interwell correlations, and three-dimensional (3D) geological models.

2.3 Section summary

This section summarizes the multistage formation of heterogeneity in low permeability reservoirs. Sedimentation, diagenesis, and fracturing jointly define a six level hierarchy from nanopores to kilometer scale reservoirs. The key implication is that heterogeneities with different scales and origins are mutually nested, and single scale observations cannot fully constrain subsurface reservoir attributes. This creates a clear need for multiscale joint characterization and physically consistent information transfer across scales.

3. Characterization: Measurement and data selection

3.1 Nanometer-micrometer scale characterization

Pore scale characterization provides information on fluid occurrence and flow in low permeability reservoirs. The main methods differ in measurement principle, resolved pore size range, and sampled volume.

(1) Gas adsorption. CO_2 adsorption characterizes pores of about 0.35-2 nm, whereas N_2 adsorption covers approximately 2-50 nm. Brunauer-Emmett-Teller, Barrett-Joyner-Halenda, and Frenkel-Halsey-Hill (FHH) analyses estimate surface area, pore size distribution, and fractal characteristics. Their outputs depend on the selected model and pore size interval; comparisons require consistent fitting procedures. Gas adsorption identifies nanopores but does not resolve 3D connectivity. Combining CO_2 and N_2 adsorption extends pore size coverage, particularly in shale and tight sandstone (Li et

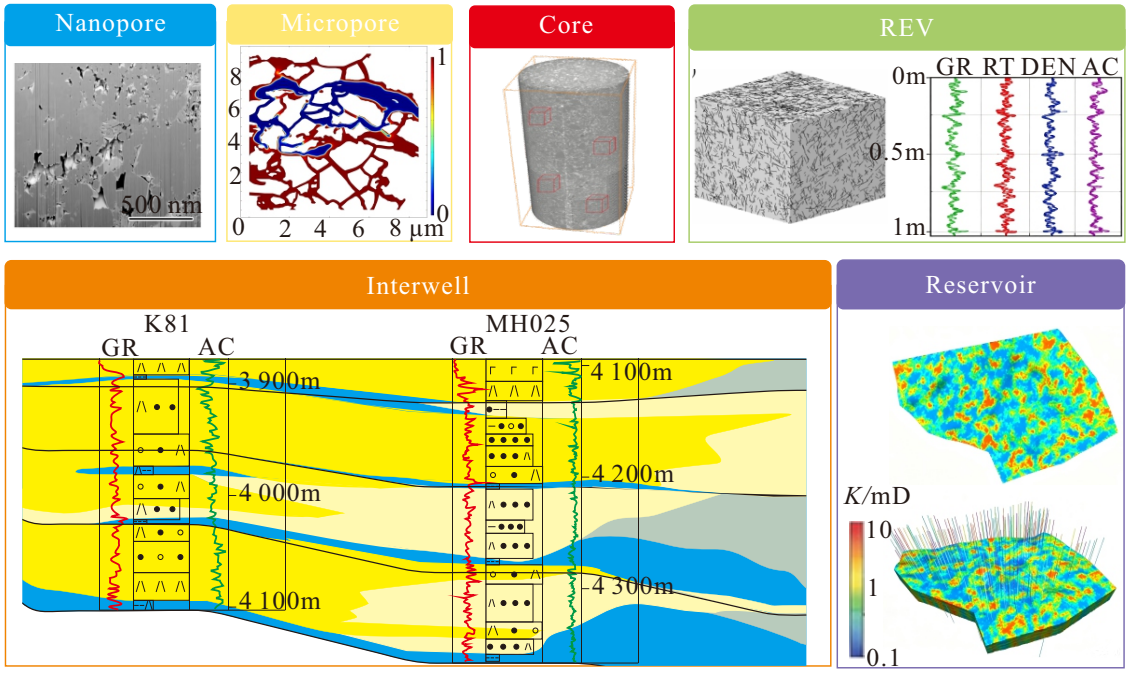


Fig. 2. Spatial hierarchy of heterogeneity from pore to reservoir scales.

al., 2024).

(2) Scanning electron microscopy (SEM) and FIB-SEM. SEM images identify pore types and mineral distributions at nanometer resolution; serial FIB-SEM imaging reconstructs 3D pore architecture. Image stitching can extend the observed range, but the resolution sample volume tradeoff remains: High resolution volumes are small and may not represent the formation (Lai et al., 2018; Blunt et al., 2025).

(3) Micro-CT. This method nondestructively images core plugs at voxel sizes of about 0.5-5 μm, resolving larger pores and microfractures but missing many submicron pores (Huang et al., 2025). Dual scale models therefore represent unresolved micropores as an effective porous medium within the resolved pore network. Image based connectivity metrics can then be evaluated within the resolution limits of the scan (Mehmani and Prodanović, 2014; Masihi et al., 2022; Bao et al., 2025a).

(4) Microfluidic rock chips. Photolithography and nanoetching reproduce selected pore-throat geometries and enable real time observation of displacement, imbibition, and gas miscibility (Godoy et al., 2025). Chip designs based on digital core images can quantify preferential pathways and local flow patterns. However, two-dimensional chips do not reproduce the full 3D mineral and fracture network. Their observations require calibration against core experiments or pore scale simulations before scale transfer (Jiang et al., 2025; Pan et al., 2026; Yang et al., 2026).

3.2 Micrometer-centimeter scale characterization

This scale covers intact core plug samples. The main objective is to evaluate pore-throat structure and fluid occurrence using complementary measurements.

(1) High-pressure mercury intrusion (HPMI). HPMI estimates pore-throat distributions over roughly 3 nm-100 μm and provides displacement and median pressures; derived fractal measures can be used to compare samples (Jouini et al., 2023). Because mercury enters through throats, the inferred pore distribution is throat constrained. Constant rate mercury intrusion can distinguish pore and throat contributions, but its pressure limit may leave the smallest pores unmeasured (Lai et al., 2018).

(2) Nuclear magnetic resonance (NMR). The transverse relaxation time (T_2) spectrum reflects fluid volume in pores of different sizes; short and long components are commonly associated with bound and more mobile fluids, respectively. A calibrated T_2 cutoff can estimate fluid fractions. NMR is nondestructive and can be cross calibrated with HPMI and adsorption data, although conversion to pore size depends on surface relaxivity and other assumptions (Fan et al., 2019). In tight sandstone, NMR derived movable fluid indicators have been related to pore-throat structure and flow capacity (Li et al., 2018). Direct analysis of echo signals has also been proposed where low signal to noise ratios make relaxation time inversion uncertain (Wu et al., 2020).

Because no single method covers the full pore size range and topology, studies combine CO_2/N_2 adsorption, HPMI, NMR, and micro-computed tomography (micro-CT), calibrating measurements within overlapping intervals before constructing a continuous distribution (Lu et al., 2024; Jamalian and Tavakoli, 2025b). The methods answer complementary questions: Adsorption extends the nanopore range, HPMI constrains throat entry sizes, NMR tracks fluid bearing pore populations, and micro-CT resolves larger pore geometry and connectivity. In the Ordos Basin, a seven method study reported abundant nanopores together with a smaller population

of large throats that influence flow (Li et al., 2026a). This observation cautions that pore abundance and flow contribution are not equivalent: The smaller throat population may be important for transport even when nanopores dominate counts or surface area. The combined measurements broaden the description, but do not eliminate uncertainty. Curve splicing can introduce systematic error because methods rely on different physical principles and calibration parameters; matched sample calibration and uncertainty reporting are therefore needed. FHH applicability and NMR-HPMI conversion, for example, depend on model choice and surface relaxivity.

3.3 Meter-kilometer scale characterization

Characterization at this scale extends core scale information to wells, interwell zones, blocks, and the reservoir. It combines static geophysical measurements with dynamic well test data.

(1) Well logging. Logs provide continuous vertical profiles and, with image logs, help identify fractures, bedding, and dissolution features (Ge et al., 2014; Bi et al., 2024). Core HPMI/NMR measurements can calibrate log based estimates of pore structure, fractal descriptors, and irreducible water saturation (Subhakar and Chandrasekhar, 2016; Matias-Gutierres et al., 2025). Machine learning interpretation may extend these relationships along wells, but reliability depends on representative training data and independent validation (Li et al., 2022b; Jamalian et al., 2025a).

(2) Seismic characterization. Seismic data constrain lateral heterogeneity between wells, although limited impedance contrast can restrict resolution in low permeability formations. Prestack inversion and amplitude versus offset attributes may improve lithology and fluid discrimination. Seismic lithology probabilities and porosity were combined with sequential Gaussian simulation to constrain interwell models (Gunning and Glinsky, 2007; Ashraf et al., 2020). Microseismic data can provide supplementary fracture information (Pi et al., 2025). These results remain dependent on well control and seismic resolution.

Frequency domain pulse well test models can interpret pressure responses between active and observation wells. Applications to channelized reservoirs, interlayer compartmentalized systems, and gas storage field cases assess spatial variation in flow barriers, preferential pathways, and transmissibility. Results depend on model assumptions, well configuration, and data quality; comparison with conventional interference test interpretations should be made for the specific field and operating conditions (Fokker et al., 2012). Tracer-based workflows provide complementary constraints for calibrating reservoir heterogeneity (Doorwar et al., 2021).

3.4 Cross scale integration of characterization data

Measurements at different scales differ in physical principle, resolution, and spatial coverage. Cross scale integration therefore requires calibration in overlapping intervals and explicit treatment of sampling and measurement uncertainty. Fig. 3 shows two complementary routes for cross scale integration. Bottom-up upscaling links pore characteristics and pore network models to well, interwell, and reservoir models. Top-down downscaling uses the large scale framework to guide parameter estimation and core scale calibration. Machine learning tools may assist scale alignment, but their outputs require geological and physical validation. Table 3 compares representative characterization methods, applicable ranges, obtainable information, and corresponding heterogeneity parameters from nanopores to interwell scales.

(1) Upscaling. Bottom-up integration calibrates overlapping pore size intervals and links SEM/FIB-SEM, micro-CT, core measurements, logs, and seismic data in sequence (Chen et al., 2024). Each step adds a different constraint: Imaging resolves geometry, core tests measure bulk response, and logs and seismic extend the interpretation spatially. Errors can accumulate across these transfers, while small samples may not be representative of the formation when extrapolated beyond the REV. Applications include linking thin section or SEM descriptors to core properties, comparing plug and full-diameter cores to assess bedding related anisotropy, and relating carbonate pore types to electrical response (Dou et al., 2011; Shedid, 2019; Tavakoli et al., 2022). These examples illustrate the transfer question of whether a feature resolved at one scale predicts an independently measured property at another, and of whether the resulting relationships, which remain lithology specific, can be recalibrated before transfer to other formations.

(2) Downscaling. Top-down workflows use seismic and logging data to define the large scale framework, then apply statistical downscaling or conditional simulation to infer finer scale properties (Table 3). Their reliability depends on well constraints, training data, and whether inferred small scale variation is geologically plausible (Cataldo and Leite, 2025).

(3) Machine learning. The bottom-up and top-down routes are complementary. Microscopic experiments constrain pore scale mechanisms, while well logs and geophysical observations constrain the larger scale framework. Their combination can connect local pore descriptions to spatially distributed reservoir properties, provided that the transfer is calibrated and its uncertainty is tracked (Mishra et al., 2020). Deep learning methods, including image reconstruction, generative adversarial networks, and diffusion models, may help align data collected at different resolutions (Davoodi et al., 2026). Their predictions must still be checked against geological evidence. In particular, reconstructed pore topology should be evaluated for geological plausibility.

3.5 Section summary

This section presents the main characterization technologies in sequence from the microscopic to the reservoir scale. Static imaging, dynamic microfluidics, core experiments, geophysical methods, and dynamic well tests provide complementary information on pore geometry, topology, petrophysical properties, and spatial architecture. Their main limitation is not a lack of measurement tools but the difficulty of fusing observations that differ in resolution, field of view, and physical measurement principle.

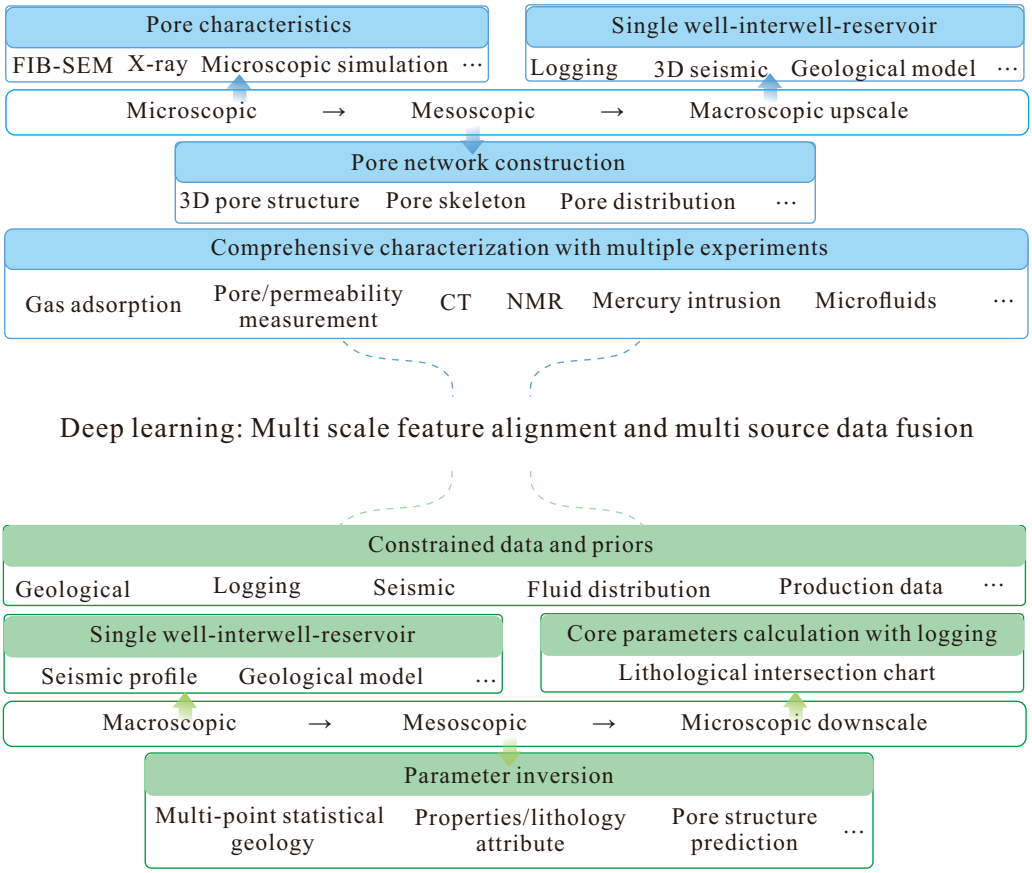


Fig. 3. Two complementary routes for cross scale integration.

Table 3. Comparison of representative multiscale characterization methods.

Method	Range	Information	Heterogeneity parameters
CO_2 adsorption	0.35-2 nm	Micropore volume, specific surface area	Micropore fractal dimension
N_2 adsorption	2-50 nm	Mesopore volume, pore size distribution	FHH fractal dimension D_1, D_2
FIB-SEM	5 nm to several μm	3D pore topological structure	Areal porosity, coordination number
micro-CT	0.5-5 μm	3D macropore network	Pore/throat topological parameters
HPMI	3 nm-100 μm	Capillary pressure, throat size distribution	Displacement pressure, fractal dimension
NMR	nm–mm	T_2 spectrum, movable fluid fraction	T_2 cutoff value, irreducible water
Well logging	dm-m	Continuous petrophysical property profile	Variation coefficient, rhythm type
Seismic	10-100 m	Lateral heterogeneous architectural pattern	Acoustic impedance variation

4. Quantification: Indicators and models

4.1 Fractal theory

Fractal theory uses statistical self similarity to describe pore geometry complexity. In low permeability reservoirs, its application depends on the measured pore size interval and fitting method (Mandelbrot, 1983). Some studies report associations between fractal descriptors and permeability, but the direction and strength vary with lithology, measurement method, and scale (Cai et al., 2020). Published models have also combined fractal descriptors with threshold pressure effects to analyze spontaneous imbibition; such results should be interpreted within their assumptions and data conditions (Zuo et al., 2024).

Monofractal methods use a single dimension to summarize geometric complexity, whereas multifractal methods describe spatial variation across pore populations. Fractal descriptors can be calculated from adsorption, HPMI, NMR, or image data using methods such as FHH, capillary bundle, relaxation spectrum, and box counting models (Liu et al., 2018; Jouini et al., 2023). The resulting values depend on the measurement principle and pore size interval; for example, adsorption and

mercury intrusion curves may show different segment boundaries (Chen et al., 2025). Fractal dimensions are therefore best used for comparisons made with consistent methods and sampling conditions (Zhang et al., 2018), rather than as interchangeable measures across scales.

Multifractal analysis extends a single fractal dimension by describing the distribution of local scaling behavior. It can distinguish spatially mixed pore populations that a single descriptor may not resolve (Jouini et al., 2022). Interpretation depends on data resolution, pore size coverage, and calibration among measurement methods.Multifractal analysis can describe spatially mixed organic pores, inorganic pores, and microfractures in shale, and has been compared with permeability and development indicators (Han et al., 2024). Its application is limited by inconsistent multi method calibration and the need to validate model specific parameter relationships for each lithology and scale.

4.2 Geostatistical method

Geostatistical modeling begins by specifying the variable Z(x) used to estimate the variogram. Continuous variables may include porosity or permeability. Facies should be represented by indicator variables rather than arbitrary numeric codes. The choice should match data distribution, sampling support, and modeling objective. The variogram is given by (Liu et al., 2018):

$$\gamma(h) = \frac{1}{2N(h)} \sum_{i=1}^{N(h)} [Z(x_i + h) - Z(x_i)]^2 \tag{1}$$

In Eq. (1), $\gamma(h)$ is semivariance at lag distance h; h is the spatial lag; $Z(x)$ is the modeled variable at location x; and $N(h)$ is the number of data pairs separated by h.

The variogram is summarized by the sill, range, and nugget, which describe overall variation, spatial correlation length, and unresolved or measurement scale variability, respectively. These parameters are estimated for the selected variable and dataset; they should not be generalized as fixed distances across formations. Kriging and sequential Gaussian simulation use the variogram to constrain spatial structure and generate multiple realizations for uncertainty assessment (Srivastava, 2013).

Two point geostatistics may miss branching or curved sedimentary bodies, whereas multiple point methods use training images to reproduce more complex architecture and connectivity (Strebelle, 2002). Performance depends on training image quality, which is governed by outcrops, dense well data, or process based models. The Lorenz coefficient can supplement model assessment when flow units and input data are representative and should be interpreted alongside spatial support and flow assumptions (Handhal et al., 2021).

4.3 Heterogeneity evaluation based on digital core

Digital core methods segment 3D images to quantify pore geometry and topology. Descriptors may include pore-throat size, coordination number, tortuosity, and shape factor. Their representativeness depends on image resolution, segmentation choices, and sampled volume (Xu et al., 2020). REV analysis should be performed for the target property and flow process, not porosity alone. The averaging volume V is increased in increments of ΔV until the selected quantity q, such as porosity, permeability tensor components, a connectivity descriptor, or effective flow response under specified boundary conditions, meets a stated dimensionless relative tolerance δ. The minimum volume satisfying this property specific criterion is reported as the REV for that quantity and condition. The units of q depend on the selected property; the relative change ratio and δ are dimensionless (Mehmani et al., 2020):

$$\left| \frac{q(V + \Delta V) - q(V)}{q(V)} \right| \leq \delta \tag{2}$$

If the estimated REV exceeds plug dimensions, the sample may not represent the target property. This can occur in low permeability rocks with abundant nanopores or long range fracture correlations, and convergence may depend on the measured quantity and boundary conditions. Dual scale pore network models address unresolved micropores by representing them as an effective medium within resolved macropores. Coupled SEM and computed tomography (CT) models have also been used to estimate tight sandstone permeability (Mehmani et al., 2020). Machine learning reconstruction and classification can extend digital core analysis, but require validation against pore connectivity and flow properties. Joint CT and HPMI measurements can link pore-throat descriptors to core scale flow response; such relationships remain conditional on imaging resolution, segmentation, and lithology (Yang et al., 2023; Xu et al., 2024).

4.4 Section summary

This section compares three mainstream quantification tools: Fractal theory, geostatistics, and digital core technology. These methods characterize microscopic pore geometry, macroscopic spatial distribution, and 3D pore networks, respectively. Fractal dimensions describe geometric complexity, variograms and related statistics describe spatial continuity, and digital core metrics describe 3D pore topology. The comparison shows that each method has a clear scale window and equally clear limitations: Fractal theory lacks unified multi experiment calibration standards, geostatistics depends strongly on training image quality, and stable REV identification remains difficult for strongly heterogeneous low permeability reservoirs.

5. Multiscale transfer mechanism

5.1 REV theory and applicability

REV theory requires a volume large enough to average pore scale variability yet small enough to preserve reservoir scale resolution (Bear, 1972). In low permeability reservoirs, unresolved nanopores, fracture correlation lengths larger than core plugs, and nonlinear flow can prevent one volume from representing all properties. Statistical elementary volumes, separate matrix/fracture continua, and local basis or discrete fracture models address different parts of this problem (Tchelepi et al., 2007).

5.2 Upscaling: From microscale to macroscale

The methods below differ in how they construct effective properties and in their sensitivity to heterogeneity and boundary conditions. Three fundamental upscaling theories are distinguished:

(1) Analytical upscaling. Volume averaging and asymptotic homogenization derive effective properties from pore scale equations (Durlofsky, 1991; Renard and de Marsily, 1997). Local conservation equations are averaged over an REV; closure relations and boundary conditions then relate averaged flux to averaged pressure gradients, yielding an effective permeability tensor. This transfer depends on the averaging volume and boundary assumptions. Coupled nonlinear processes can invalidate a single rate independent effective property (Whitaker, 1986):

$$\nabla \cdot \left(\frac{K}{\mu} (\nabla p - \rho g) \right) = 0 \tag{3}$$

$$\langle v \rangle = -\frac{\langle K \rangle}{\mu} (\nabla \langle p \rangle - \rho g) \tag{4}$$

Here, K is permeability, $\langle \cdot \rangle$ denotes volume averaging over the REV, v is flow velocity, p is pressure, μ is dynamic viscosity, ρ is fluid density, and g is gravitational acceleration.

Rate sensitive upscaling represents the dependence of effective two phase properties on displacement rate and should be calibrated over target rate and saturation ranges. The multiscale finite volume method uses local basis functions to transfer fine scale permeability contrasts to coarse grids (Jenny et al., 2003). The principal error sources are unresolved connected channels or fractures, coarse grid resolution, and boundary condition mismatch. Applicability should be assessed by comparing pressure and flux with fine grid solutions across representative heterogeneity levels.

(2) Numerical upscaling. Fine grid flow is solved within coarse blocks to estimate effective properties (Arbogast, 2004). For two phase flow, relative permeability may depend on displacement rate and require iterative calibration. Threshold pressure effects can make equivalent properties grid size dependent (Cai, 2014). Two stage coarsening from core to geological model and then simulation grid can reduce computational cost, but accuracy should be reported for the tested model, grid, and flow conditions (Lohne et al., 2006; Sharifi and Kelkar, 2012).

(3) Computational homogenization. Multiscale finite element, finite volume, and variational methods use local basis functions to represent fine scale effects on coarse grids. The multiscale finite volume method constructs basis functions from local flow solutions and can represent strong permeability contrasts. Grid design, connectivity, boundary conditions, and nonlinear terms such as threshold pressure affect convergence and error. Validation against fine scale pressure and flux solutions is needed for each intended heterogeneity range (Møyner and Lie, 2016).

Published workflows link pore structure, core measurements, well logs, seismic data, and fracture models, but each requires a defined transfer target and field specific calibration. Examples include: (1) relating pore structure descriptors to porosity and permeability, with calibration against core measurements (Rahimi et al., 2018); (2) combining well logs and seismic attributes to constrain lithology and physical property models (Peçanha et al., 2019); (3) using gravel content and grain size as mesoscopic descriptors and comparing core ultrasonic measurements with well log responses (Liu et al., 2022); (4) coupling pore and fracture network descriptions with discrete fracture models to assess scale dependent controls on shale gas productivity (Tian et al., 2022); (5) integrating core measurements to map capillary heterogeneity (Hingerl et al., 2016); and (6) transferring digital core flow descriptors to reservoir simulation with uncertainty assessed by sampling and probability analysis (Aslannezhad et al., 2025).

5.3 Nonlinear transfer mechanisms in low permeability reservoirs

At pore scale, interfacial forces and geometric constraints can produce nonlinear flow responses that complicate transfer to reservoir models (Cai and Hu, 2019). Their importance depends on lithology, fluid properties, pressure, and pore size distribution.

(1) Threshold pressure gradient effect. As shown in Fig. 4, low permeability flow may require a critical pressure gradient because of boundary layer yield stress, nanopore interfacial forces, or non Newtonian behavior (Cai, 2014). Experiments and coupled models have described a dynamic resistance gradient that varies with displacement pressure, rather than a fixed rock property (Sun et al., 2019). Therefore, a laboratory threshold measured at one condition may not transfer directly to reservoir simulation and may misrepresent flow capacity far from the well. Threshold pressure behavior departs from classical Darcy flow below a condition dependent pressure gradient. The response should be measured over relevant fluid, stress, and rate conditions; a single threshold value should not be treated as a universal rock property.

(2) Scale differentiation of boundary layer and movable fluids (Fig. 5). Adsorbed boundary layers reduce effective flow diameter, with a larger relative effect in smaller pore-throat (Sun et al., 2019). NMR derived movable fluid indicators have been related to pore structure in tight sandstone, but the relationship depends on surface relaxivity, cutoff selection, and sample calibration (Li et al., 2018). Equivalent permeability may vary with pressure gradient, so core scale parameters require validation before upscaling.

(3) Stress sensitivity effect. As shown in Fig. 6, Effective stress changes can close or deform pore-throat and alter permeability. The magnitude and direction depend on lithology, stress path, confining pressure, and measurement protocol; core stress sensitivity curves require broader sampling before reservoir scale transfer (Jones and Owens, 1980; Cai et al., 2020).

(4) Gas slippage effect (Fig. 7). Gas slippage can increase apparent gas permeability relative to liquid permeability in small gas filled throats, especially at lower pressure. Its contribution should be evaluated using the pore size distribution and pressure range of the target formation (Jones and Owens, 1980; Javadpour et al., 2021).

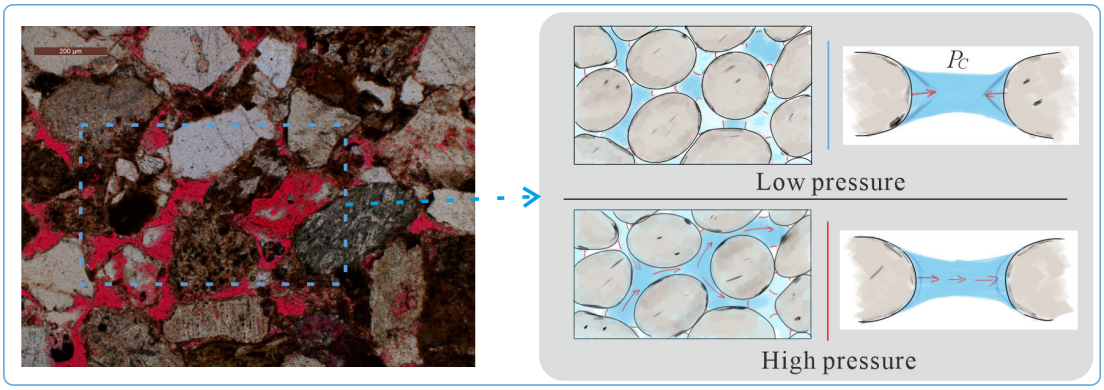


Fig. 4. Schematic of threshold pressure gradient. The diagrams illustrate how pressure conditions influence gas flow through pore-throat.

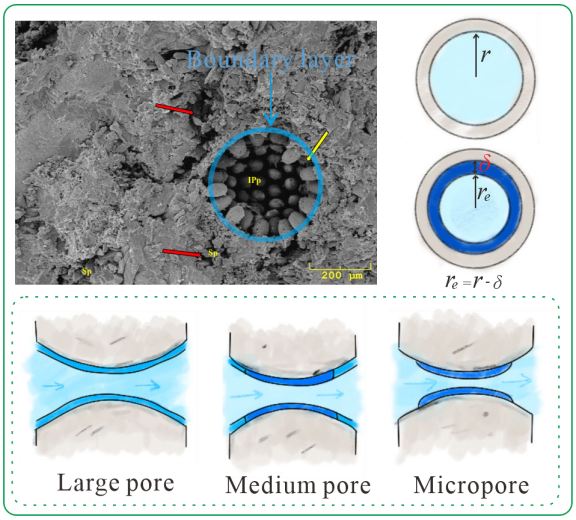


Fig. 5. Schematic of scale differentiation of boundary layer and movable fluids. As pore size decreases, the boundary layer occupies a greater proportion of the pore space.

(5) Fracture matrix fluid exchange effect. In fractured reservoirs, capillary imbibition transfers fluid between matrix and fractures. The response depends on pore structure, wettability, fracture geometry, and boundary conditions. Transfer from pore and network observations to core or reservoir scale recovery therefore requires calibration under representative conditions (Zuo et al., 2024; Zhang et al., 2025; Liu et al., 2026).

5.4 Evolution of dynamic heterogeneity during reservoir development

During production and injection, stress changes, fluid redistribution, particle migration, and geochemical reactions can alter pore-throat structure, connectivity, and relative permeability. Depletion may compact the matrix or close fractures; injection may reopen conductive pathways, while dissolution or precipitation modifies pore geometry. The dominant process and its direction depend on rock type, fluid chemistry, stress path, and operating conditions (Wu et al., 2021; Hui et al., 2024; Bao et al., 2025b; Cheng et al., 2026).

Dynamic heterogeneity can be tracked with time lapse measurements of permeability, pore structure, fracture connectivity, and fluid saturation, together with pressure and production/injection data. Coupled models should include processes relevant to the target lithology and be calibrated against laboratory or field observations.

6. Conclusions and research priorities

This study links the genetic origins of heterogeneity with multiscale measurement, quantitative description, and scale transfer. Four bottlenecks limit engineering application: Cross method calibration and uncertainty; property and rate dependent nonlinear upscaling; time evolving heterogeneity under coupled stress, fluid, and chemical processes; and limited experimental coverage and computational efficiency.

Research should prioritize (1) matched sample calibration and uncertainty propagation across measurement methods; (2) flow linked heterogeneity indicators tested against independent measurements; (3) nonlinear upscaling validated across lithologies, heterogeneity levels, and operating conditions; and (4) time lapse datasets and coupled models that track stress, fluid, and chemical evolution. Each workflow should distinguish transferable mechanisms from parameters requiring local calibration, and conclusions should be tested against independent core and field data.

Acknowledgments

This research was financially supported by the National Natural Science Foundation of China (No. 52674070) and National Science and Technology Major Project for New-type Oil and Gas Exploration and Development (No. 2025ZD1401405).

Conflicts of interest

The authors declare no competing interest.

Open Access This article is distributed under the terms and conditions of the Creative Commons Attribution (CC BY-NC-ND) license, which permits unrestricted use, distribution, and reproduction in any medium, provided the original work is properly cited.

References

Alkareemawi, A. M. M., Hasnan, H. K., Mustapha, K. A. Multi-scale characterization of carbonate reservoir qual-

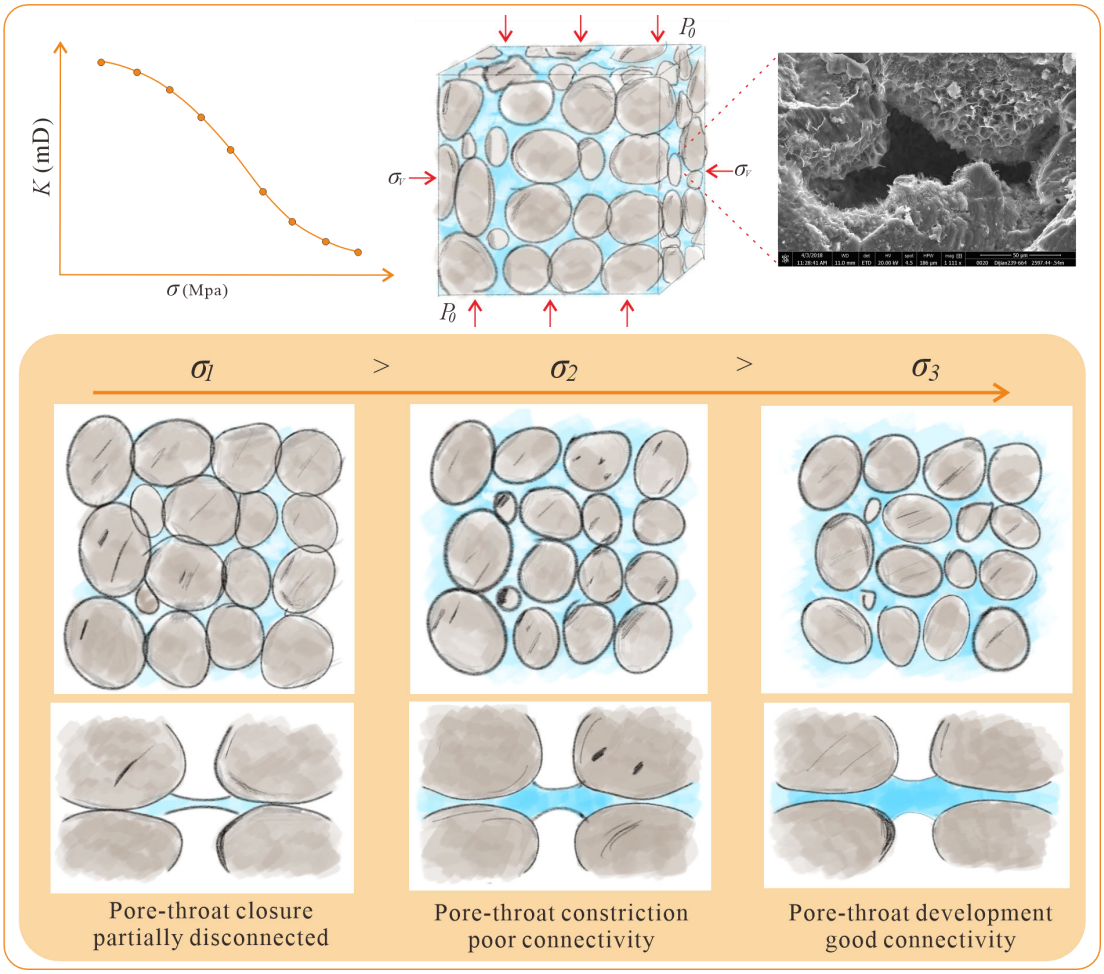


Fig. 6. Schematic of stress sensitivity. Increasing stress promotes pore-throat closure and constriction, reducing connectivity and permeability.

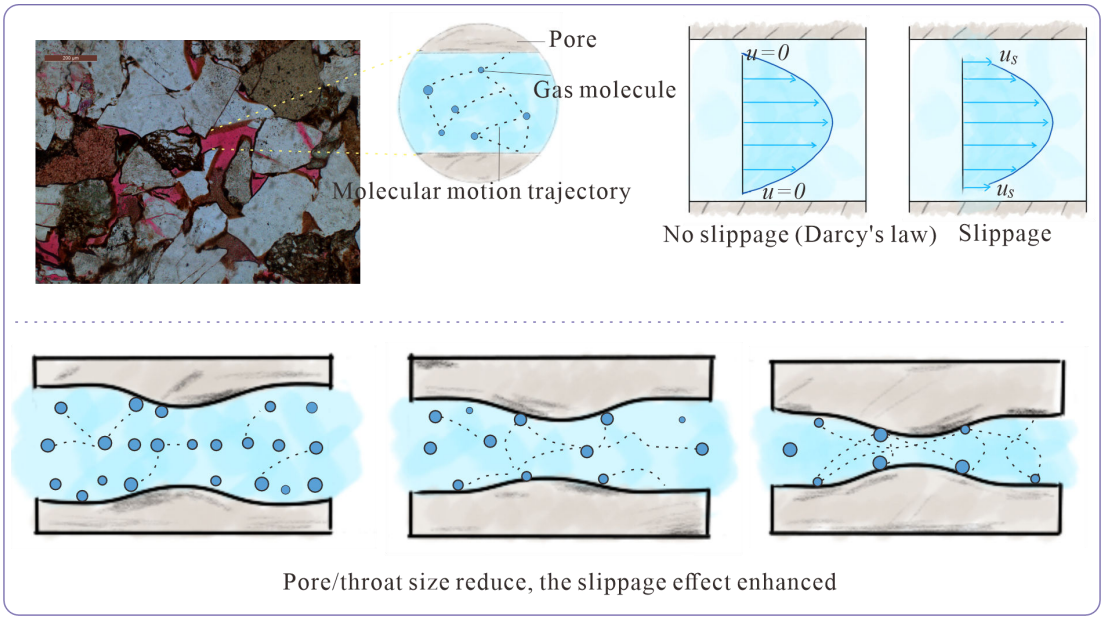


Fig. 7. Schematic of gas slippage. The slippage effect becomes more pronounced as the pore-throat size decreases.

ity, diagenesis, and microfacies in the upper cretaceous khasib formation, South Iraq. Journal of African Earth Sciences, 2025, 232: 105819.

Arbogast, T. Analysis of a two-scale, locally conservative subgrid upscaling for elliptic problems. SIAM Journal on Numerical Analysis, 2004, 42(2): 576-598.

Ashraf, U., Zhang, H., Anees, A., et al. Controls on reservoir heterogeneity of a shallow-marine reservoir in Sawan Gas Field, SE Pakistan: Implications for reservoir quality prediction using acoustic impedance inversion. Water, 2020, 12(11): 2972.

Aslannezhad, M., Sayyafzadeh, M., Tang, D., et al. Application of digital core analysis to improve reservoir characterisation and modelling: The Otway formation as a case study. International Journal of Greenhouse Gas Control, 2025, 141: 104316.

Bao, J., Du, J., Zhan, S., Wang, L., Luo, Y. A molecular perspective on the microscopic mechanisms of CO_2 injection and water films in fluid transport and enhanced oil recovery. Advances in Geo-Energy Research, 2025a, 16(3): 288-292.

Bao, P., Hui, G., Hu, Y., et al. Comprehensive characterization of hydraulic fracture propagations and prevention of pre-existing fault failure in Duvernay shale reservoirs. Engineering Failure Analysis, 2025b, 173: 109461.

Bear, J. Dynamics of Fluids in Porous Media. New York, USA, American Elsevier Publishing Company, 1972.

Bi, X., Li, J., Lian, C. A comprehensive logging evaluation method for identifying high-quality shale gas reservoirs based on multifractal spectra analysis. Scientific Reports, 2024, 14(1): 26107.

Blunt, M. J., Sun, S., Boone, M. A., Zhang, L., Cai, J. Digital rock physics and fluid flow in the context of the energy transition. Advances in Geo-Energy Research, 2025, 18(3): 299-302.

Bultreys, T., De Boever, W., Cnudde, V. Imaging and image-based fluid transport modeling at the pore scale in geological materials: A practical introduction to the current state-of-the-art. Earth-Science Reviews, 2016, 155: 93-128.

Cai, J. A fractal approach to low velocity non-Darcy flow in a low permeability porous medium. Chinese Physics B, 2014, 23(4): 044701.

Cai, J., Hu, X. Petrophysical Characterization and Fluids Transport in Unconventional Reservoirs. Amsterdam, The Netherlands, Elsevier, 2019.

Cai, J., Xia, Y., Lu, C., et al. Creeping microstructure and fractal permeability model of natural gas hydrate reservoir. Marine and Petroleum Geology, 2020, 115: 104282.

Cataldo, R. A., Leite, E. P. Integrated machine learning workflow for 3D pore type modeling in the pre-salt carbonates of the Tupi Field, Santos Basin. Journal of Applied Geophysics, 2025, 237: 105689.

Chen, S., Liu, D., Wang, Y., et al. A comparative analysis of mercury intrusion and nitrogen adsorption methods for multifractal characterization of shale reservoirs in northern Songliao Basin. Scientific Reports, 2025, 15(1): 7866.

Chen, X., Zhou, K., Jiang, P., et al. Identification, characterization, and up-scaling of pore structure facies in the low permeability reservoirs: Insight into reservoir quality evaluation and sweet-spots analysis. Marine and Petroleum Geology, 2024, 162: 106646.

Cheng, C., Hui, G., Chen, Z. Energy-efficient fracturing based on stress-coupled perforation. Petroleum Science, 2026, 23(8): 4873-4890.

Correia, M. G., Maschio, C., Schiozer, D. J. Development of complex layered and fractured reservoir models for reservoir simulation. Journal of the Brazilian Society of Mechanical Sciences and Engineering, 2017, 39(1): 219-233.

Davoodi, S., Wood, D. A., Al-Shargabi, M., et al. Emerging applications of physics-informed and physics-guided machine learning in geoenergy science: A review. Communications in Nonlinear Science and Numerical Simulation, 2026, 154: 109551.

Doorwar, S., Purswani, P., Ambastha, A., et al. Application of tracer-based workflow for calibrating reservoir heterogeneity. SPE Reservoir Evaluation & Engineering, 2021, 24(3): 603-618.

Dou, Q., Sun, Y., Sullivan, C. Rock-physics-based carbonate pore type characterization and reservoir permeability heterogeneity evaluation, upper San Andres reservoir, Permian Basin, west Texas. Journal of Applied Geophysics, 2011, 74(1): 8-18.

Durlofsky, L. J. Numerical calculation of equivalent grid block permeability tensors for heterogeneous porous media. Water Resources Research, 1991, 27(5): 699-708.

Durlofsky, L. J. Coarse scale models of two phase flow in heterogeneous reservoirs: Volume averaged equations and their relationship to existing upscaling techniques. Computational Geosciences, 1998, 2: 73-92.

Fan, X., Wang, G., Li, Y., et al. Pore structure evaluation of tight reservoirs in the mixed siliciclastic-carbonate sediments using fractal analysis of NMR experiments and logs. Marine and Petroleum Geology, 2019, 109: 484-493.

Farhoodi, S., Sadeghnejad, S., Saeedi Dehaghani, A. H. Simultaneous effect of geological heterogeneity and condensate blockage on well test response of gas condensate reservoirs. Journal of Natural Gas Science and Engineering, 2019, 66: 192-206.

Fokker, P. A., Salina Borello, E., Serazio, C., et al. Estimating reservoir heterogeneities from pulse testing. Journal of Petroleum Science and Engineering, 2012, 86-87: 15-26.

Gerritsen, M. G., Durlofsky, L. J. Modeling fluid flow in oil reservoirs. Annual Review of Fluid Mechanics, 2005, 37: 211-238.

Ge, X., Fan, Y., Zhu, X., et al. A method to differentiate degree of volcanic reservoir fracture development using conventional well logging data–an application of kernel principal component analysis (KPCA) and multifractal detrended fluctuation analysis (MFDFA). IEEE Journal of Selected Topics in Applied Earth Observations and Remote Sensing, 2014, 7(12): 4972-4978.

Godoy, P. A., Orujov, A., Pérez Gramatges, A., et al. Rock-

on-a-chip: A novel method for designing representative microfluidic platforms based on real rock structures and pore network modelling. Lab on a Chip, 2025, 25(13): 3109-3122.

Gunning, J., Glinsky, M. E. Detection of reservoir quality using Bayesian seismic inversion. Geophysics, 2007, 72(3): R37-R49.

Han, Y., Jiang, Z., Liang, Z., et al. Study on the multifractal characterization and seepage of the shale matrix: A case study of the Longmaxi Formation in southwestern Sichuan Basin, China. Geoenergy Science and Engineering, 2024, 238: 212924.

Handhal, A. M., Hussein, A. A., Al-Abadi, A. M., et al. Spatial modeling of hydrocarbon productivity in the Nahr Umr Formation at the Luhais Oil Field, Southern Iraq. Natural Resources Research, 2021, 30(1): 765-787.

Hingerl, F. F., Yang, F., Pini, R., et al. Characterization of heterogeneity in the Heletz sandstone from core to pore scale and quantification of its impact on multi-phase flow. International Journal of Greenhouse Gas Control, 2016, 48: 69-83.

Huang, R., Qiao, D., Hui, G., et al. A fracture extraction method for full-diameter core CT images based on semantic segmentation. Processes, 2025, 13(7): 2221.

Hui, G., Chen, S., He, Y., et al. Machine learning-based production forecast for shale gas in unconventional reservoirs via integration of geological and operational factors. Journal of Natural Gas Science and Engineering, 2021, 94: 104045.

Hui, G., Chen, S., Gu, F. Strike-slip fault reactivation triggered by hydraulic-natural fracture propagation during fracturing stimulations near Clark Lake, Alberta. Energy & Fuels, 2024, 38(19): 18547-18555.

Hui, G., Ren, Y., Bi, J., et al. Artificial intelligence applications and challenges in oil and gas exploration and development. Advances in Geo-Energy Research, 2025, 17(3): 179-183.

Jamalian, A., Rabbani, A. R., Asemani, M. Integrated clustering and electrofacies analysis for reservoir quality and heterogeneity assessment: A case study from a Southern Iranian Gas Field. Natural Resources Research, 2025a, 34(4): 2189-2205.

Jamalian, A., Tavakoli, V. Integrating routine and novel methods for a comprehensive analysis of heterogeneity in Persian Gulf's Permian-Triassic carbonate reservoirs. Marine and Petroleum Geology, 2025b, 173: 107277.

Javadpour, F., Singh, H., Rabbani, A., et al. Gas flow models of shale: A review. Energy & Fuels, 2021, 35(4): 2999-3010.

Jenny, P., Lee, S. H., Tchelepi, H. A. Multi-scale finite-volume method for elliptic problems in subsurface flow simulation. Journal of Computational Physics, 2003, 187(1): 47-67.

Jia, C., Zheng, M., Zhang, Y. Unconventional hydrocarbon resources in China and the prospect of exploration and development. Petroleum Exploration and Development, 2012, 39(2): 139-146.

Jia, C. Breakthrough and significance of unconventional oil and gas to classical petroleum geology theory. Petroleum Exploration and Development, 2017, 44(1): 1-10.

Jiang, W., Liu, G., Pu, X., et al. Microfluidic experimental study on oil phase mobility during CO_2-hydrocarbon gas injection in tight oil reservoirs. ACS Omega, 2025, 10(45): 54660-54670.

Jones, F. O., Owens, W. W. A laboratory study of low-permeability gas sands. Journal of Petroleum Technology, 1980, 32(9): 1631-1640.

Jouini, M. S., Bouchaala, F., Riahi, M. K., et al. Multifractal analysis of reservoir rock samples using 3D X-ray micro computed tomography images. IEEE Access, 2022, 10: 67898-67909.

Jouini, M. S., Alabere, A. O., Alsuwaidi, M., et al. Experimental and digital investigations of heterogeneity in lower cretaceous carbonate reservoir using fractal and multifractal concepts. Scientific Reports, 2023, 13(1): 20306.

Kim, T. H., Schechter, D. S. Estimation of fracture porosity of naturally fractured reservoirs with no matrix porosity using fractal discrete fracture networks. SPE Reservoir Evaluation & Engineering, 2009, 12(2): 232-242.

Kulga, B., Artun, E., Ertekin, T. Characterization of tight-gas sand reservoirs from horizontal-well performance data using an inverse neural network. Journal of Natural Gas Science and Engineering, 2018, 59: 35-46.

Lai, J., Wang, G., Wang, Z., et al. A review on pore structure characterization in tight sandstones. Earth-Science Reviews, 2018, 177: 436-457.

Li, C., Su, D., Chen, P., et al. Multiscale microscopic pore structure characterization and storage-flow coupling mechanisms in ultra-low permeability tight sandstone reservoirs. Scientific Reports, 2026a, 16(1): 14811.

Li, G., Xian, C., Liu, H. A "One Engine with Six Gears" system engineering methodology for the economic development of unconventional oil and gas in China. Engineering, 2022a, 18: 105-115.

Li, H., He, S., Radwan, A. E., et al. Quantitative analysis of pore complexity in lacustrine organic-rich shale and comparison to marine shale: Insights from experimental tests and fractal theory. Energy & Fuels, 2024, 38(17): 16171-16188.

Li, H., Duan, H., Qin, Q., et al. Characteristics and distribution of tectonic fracture networks in low permeability conglomerate reservoirs. Scientific Reports, 2025a, 15(1): 5914.

Li, H., Qin, Q., Li, C., et al. Quantitative characterization of complex multi-scale fractures in low-permeable sandstone reservoir: Insights from geological and mathematical approach. Geomechanics and Geophysics for Geo-Energy and Geo-Resources, 2026b, 12(1): 39.

Li, P., Sun, W., Wu, B., et al. Occurrence characteristics and influential factors of movable fluids in pores with different structures of Chang 63 reservoir, Huaqing Oilfield, Ordos Basin, China. Marine and Petroleum Geology, 2018, 97: 480-492.

Li, T., Li, Q., Hu, Y., et al. Quantitative characterization of irregular microfracture network and its effect on the

permeability of porous media. Petroleum Exploration and Development, 2021, 48(2): 430-441.

Li, Y., Hui, G., Zhang, Z., et al. Insights on shale gas production prediction via combining multimodal machine learning with deterministic geological modeling. Paper SPE 229353 Presented at the ADIPEC, Abu Dhabi, United Arab Emirates, 3-6 November, 2025b.

Li, Y., Luo, M., Ma, S., et al. Massive spatial well clustering based on conventional well log feature extraction for fast formation heterogeneity characterization. Lithosphere, 2022b, 2022(Special 12): 7260254.

Liu, J., Ge, H., Mou, S., et al. Characterization of mesostructure of glutenite reservoirs by ultrasonic characteristics and the velocity heterogeneity. Journal of Petroleum Science and Engineering, 2022, 208: 109436.

Liu, K., Ostadhassan, M., Zou, J., et al. Multifractal analysis of gas adsorption isotherms for pore structure characterization of the Bakken Shale. Fuel, 2018, 219: 296-311.

Liu, Q., Wang, Q., Liang, B., et al. Multi-scale studies of oil-water imbibition mechanism on complex pore structures and mixed-wettability: A recent 10-year review. Scientific Reports, 2026, 16(1): 11979.

Lohne, A., Virnovsky, G., Durlofsky, L. J. Two-stage upscaling of two-phase flow: From core to simulation scale. SPE Journal, 2006, 11(3): 304-316.

Lu, H., Li, Q., Yue, D., et al. Multi-scale pore structure heterogeneity in tuff reservoirs investigated with multi-experimental method and fractal dimensions in Chang 7 Formation, Southern Ordos Basin. Journal of Earth Science, 2024, 35(2): 666-686.

Malki, M. L., Saberi, M. R., Kolawole, O., et al. Underlying mechanisms and controlling factors of carbonate reservoir characterization from rock physics perspective: A comprehensive review. Geoenergy Science and Engineering, 2023, 226: 211793.

Mandelbrot, B. B. The Fractal Geometry of Nature. San Francisco, USA, W. H. Freeman, 1983.

Masihi, M., Shams, R., King, P. R. Pore level characterization of micro-CT images using percolation theory. Journal of Petroleum Science and Engineering, 2022, 211: 110113.

Matias-Gutierres, S., García-Otamendi, E. I., Sánchez-Chávez, H. D., et al. Fractal scaling of storage capacity fluctuations in well logs from southeastern Mexican reservoirs. Fractal and Fractional, 2025, 9(8): 548.

Mehmani, A., Prodanović, M. The effect of microporosity on transport properties in porous media. Advances in Water Resources, 2014, 63: 104-119.

Mehmani, A., Kelly, S., Torres-Verdín, C. Leveraging digital rock physics workflows in unconventional petrophysics: A review of opportunities, challenges, and benchmarking. Journal of Petroleum Science and Engineering, 2020, 190: 107083.

Mishra, A., Kurtev, K. D., Haese, R. R. Composite rock types as part of a workflow for the integration of mm-to cm-scale lithological heterogeneity in static reservoir models. Marine and Petroleum Geology, 2020, 114: 104240.

Møyner, O., Lie, K. A. A multiscale restriction-smoothed basis method for high contrast porous media represented on unstructured grids. Journal of Computational Physics, 2016, 304: 46-71.

Pan, X., Sun, L., Xiao, H., et al. Nanofluidic replication of reservoir pore networks on silicon chips: New insights of the miscibility of CO_2-alkane systems in nano-confined spaces. Journal of CO_2 Utilization, 2026, 104: 103324.

Peçanha, A. A., Lupinacci, W. M., Ferreira, D. J. A., et al. A workflow for reservoir characterization applied to presalt coquinas from the Linguado Field, Campos Basin, Brazil. Journal of Petroleum Science and Engineering, 2019, 183: 106451.

Pi, Z., Zhang, Y., Hui, G., et al. Comprehensive characterization of the unconventional fracture networks via fiber optic tools and microseismicity analysis. Paper SPE 225334 Presented at SPE Advances in Integrated Reservoir Modelling and Field Development Conference and Exhibition, Abu Dhabi, UAE, 2-4 June, 2025.

Qiao, J., Zeng, J., Xia, Y., et al. A three dimensional visualized physical simulation for natural gas charging in the micro-nano pore system. Petroleum Exploration and Development, 2022, 49(2): 349-362.

Rahimi, R., Bagheri, M., Masihi, M. Characterization and estimation of reservoir properties in a carbonate reservoir in Southern Iran by fractal methods. Journal of Petroleum Exploration and Production Technology, 2018, 8(1): 31-41.

Ren, B., Trevisan, L. Characterization of local capillary trap clusters in storage aquifers. Energy, 2020, 193: 116795.

Renard, P., de Marsily, G. Calculating equivalent permeability: A review. Advances in Water Resources, 1997, 20(5-6): 253-278.

Sadeghnejad, S., Enzmann, F., Kersten, M. Digital rock physics, chemistry, and biology: Challenges and prospects of pore-scale modelling approach. Applied Geochemistry, 2021, 131: 105028.

Sharifi, M., Kelkar, M. New upgridding method to capture the dynamic performance of the fine scale heterogeneous reservoir. Journal of Petroleum Science and Engineering, 2012, 86-87: 225-236.

Shedid, S. A. Prediction of vertical permeability and reservoir anisotropy using coring data. Journal of Petroleum Exploration and Production Technology, 2019, 9(3): 2139-2143.

Srivastava, R. M. Geostatistics: A toolkit for data analysis, spatial prediction and risk management in the coal industry. International Journal of Coal Geology, 2013, 112: 2-13.

Strebelle, S. Conditional simulation of complex geological structures using multiple-point statistics. Mathematical Geology, 2002, 34: 1-21.

Su, X., Ren, B., Huang, Z. Permeability analysis of fractured-vuggy carbonate reservoirs based on fractal theory. Fractals, 2022, 30(7): 2250144.

Subhakar, D., Chandrasekhar, E. Reservoir characterization using multifractal detrended fluctuation analysis of geophysical well-log data. Physica A: Statistical Mechanics and its Applications, 2016, 445: 57-65.

Sun, Z., Ma, B., Li, F. Mechanism and characteristics of non-

linear flow in porous media of low permeability reservoir. Journal of Southwest Petroleum University (Science & Technology Edition), 2019, 41(2): 109-117. (in Chinese)

Tavakoli, V., Hassani, D., Rahimpour-Bonab, H., et al. How petrophysical heterogeneity controls the saturation calculations in carbonates, the Barremian-Aptian of the central Persian Gulf. Journal of Petroleum Science and Engineering, 2022, 208: 109568.

Tchelepi, H. A., Jenny, P., Lee, S. H., et al. Adaptive multiscale finite-volume framework for reservoir simulation. SPE Journal, 2007, 12(2): 188-195.

Tian, J., Liu, J., Elsworth, D., et al. Shale gas production from reservoirs with hierarchical multiscale structural heterogeneities. Journal of Petroleum Science and Engineering, 2022, 208: 109380.

Veloso, F. M. L., Navarrete, R., Soria, A. R., et al. Sedimentary heterogeneity and petrophysical characterization of Barremian tsunami and barrier island/inlet deposits: The Aliaga outcrop as a reservoir analogue (Galve sub-basin, eastern Spain). Marine and Petroleum Geology, 2016, 73: 188-211.

Wang, H., Ma, F., Tong, X., et al. Assessment of global unconventional oil and gas resources. Petroleum Exploration and Development, 2016, 43(6): 925-940.

Wang, Y., Blunt, M. J., Armstrong, R. T., et al. Deep learning in pore scale imaging and modeling. Earth-Science Reviews, 2021, 215: 103555.

Whitaker, S. Flow in porous media I: A theoretical derivation of Darcy's law. Transport in Porous Media, 1986, 1(1): 3-25.

Wu, B., Xie, R., Wang, X., et al. Characterization of pore structure of tight sandstone reservoirs based on fractal analysis of NMR echo data. Journal of Natural Gas Science and Engineering, 2020, 81: 103483.

Wu, M., Wang, W., Song, Z., et al. Exploring the influence of heterogeneity on hydraulic fracturing based on the combined finite-discrete method. Engineering Fracture Mechanics, 2021, 252: 107835.

Xi, K., Cao, Y., Liu, K., et al. Geochemical constraints on the origins of calcite cements and their impacts on reservoir heterogeneities: A case study on tight oil sandstones of the Upper Triassic Yanchang Formation, southwestern Ordos Basin, China. AAPG Bulletin, 2019, 103(10): 2447-2485.

Xu, T., Liang, X., Xia, Y., et al. Performance evaluation of the Habanero enhanced geothermal system, Australia: Optimization based on tracer and induced micro-seismicity data. Renewable Energy, 2022, 181: 1197-1208.

Xu, Z., Lin, M., Jiang, W., et al. Identifying the comprehensive pore structure characteristics of a rock from 3D images. Journal of Petroleum Science and Engineering, 2020, 187: 106764.

Xu, Z., Lin, M., Jiang, W., et al. A pore network-based multiscale coupled model for rapid permeability prediction of tight sandstone gas. Marine and Petroleum Geology, 2024, 160: 106600.

Yang, J., Moradpour, N., Au-Yeung, L., et al. Lab-on-a-chip insights: Advancing subsurface flow applications in carbon management and hydrogen storage. Lab on a Chip, 2026, 26(5): 1352-1393.

Yang, Y. B., Xiao, W. L., Zheng, L. L., et al. Pore throat structure heterogeneity and its effect on gas-phase seepage capacity in tight sandstone reservoirs: A case study from the Triassic Yanchang Formation, Ordos Basin. Petroleum Science, 2023, 20(5): 2892-2907.

Zhang, K., Pang, X., Zhao, Z., et al. Pore structure and fractal analysis of Lower Carboniferous carbonate reservoirs in the Marsel area, Chu-Sarysu basin. Marine and Petroleum Geology, 2018, 93: 451-467.

Zhang, Y., Pi, Z., Hui, G., et al. Experimental research on surfactant flooding and design of integrated schemes for energy storage fracturing and production in tight sandstone reservoirs. Processes, 2025, 13(12): 4031.

Zuo, M. S., Chen, H., Liu, X. L., et al. Fractal model of spontaneous imbibition in low-permeability reservoirs coupled with heterogeneity of pore seepage channels and threshold pressure. Petroleum Science, 2024, 21(2): 1002-1017.